

TN 1254

~~CONFIDENTIAL~~

# NATIONAL ADVISORY COMMITTEE FOR AERONAUTICS

TECHNICAL NOTE

No. 1254

ITERATIVE INTERFERENCE METHODS IN THE DESIGN  
OF THIN CASCADE BLADES

By Leo Diesendruck

Langley Memorial Aeronautical Laboratory  
Langley Field, Va.



Washington

May 1947

NACA LIBRARY  
LANGLEY MEMORIAL AERONAUTICAL  
LABORATORY  
Langley Field, Va.



3 1176 01433 3398

## NATIONAL ADVISORY COMMITTEE FOR AERONAUTICS

TECHNICAL NOTE NO. 1254

ITERATIVE INTERFERENCE METHODS IN THE DESIGN  
OF THIN CASCADE BLADES

By Leo Diesendruck

## SUMMARY

The iterative interference method given in NACA TN No. 1252 is applied to the solution of the following three problems concerning the design of cascades:

(1) Determination of the shape and setting of thin (zero thickness) blades with a prescribed type of vortex distribution and total vortex strength in a cascade of given solidity for a given direction of the mean flow.

(2) Determination of the shape and setting of thin blades with certain prescribed types of pressure distributions over one surface and prescribed total vortex strength in a cascade of given solidity for a given direction of the mean flow.

(3) Determination of the blade setting for a cascade of given airfoil shape and solidity that, for a given direction of the incoming (upstream) flow, will provide the front stagnation point exactly at the leading edge.

A modification of the basic procedure of TN No. 1252 is also described, in which the direction of the incoming flow, rather than the direction of the mean flow, is specified.

## INTRODUCTION

In reference 1, an iterative interference method was described for calculating the potential flow on an airfoil in cascade. The method, which makes use of charts originally employed by Betz in a similar study (reference 2), evaluates the flow at each airfoil as the sum of two components - that due to the uniform mean, or "free stream" flow, and the interference flow induced by the presence of

all the other airfoils of the cascade. As was indicated in reference 1, such an approach provides considerable flexibility and permits the solution, with reasonable facility, of certain cascade problems that would be very difficult by the usual methods that seek directly the conformal transformation of the cascade to a circle. In the present paper the solutions of three such problems are described and an example of each is given. Two of the problems concern the design of thin (zero thickness) airfoil cascades having prescribed types of vorticity distribution or pressure distribution along the blade. The other problem is the determination of the blade setting, for a cascade of given airfoil shape and solidity, that, for a given direction of the incoming (upstream) flow, will provide the front stagnation point exactly at the leading edge. A modification of the basic procedure of reference 1 is also described in which the direction of the incoming flow, rather than the direction of the mean flow, is specified.

Basic concepts and techniques are given in reference 1, and detailed discussions are accordingly given herein only for those parts of the procedure that are not contained in reference 1.

#### SYMBOLS

$V$	flow velocity
$u$	component of flow velocity parallel to stagger line
$v$	component of mean flow velocity normal to stagger line
$\beta$	blade angle, angle between chord and normal to cascade axis
$\alpha$	angle between chord and velocity indicated by subscript
$\psi$	stream function
$\Phi$	velocity potential
$\Gamma$	circulation required to provide stagnation point at trailing edge
$\Gamma^*$	circulation required to provide stagnation point at leading edge
$\gamma$	circulation per unit arc length
$x, y$	coordinates of point on arc

- $\theta$  angular position of point on arc  
 $\rho$  radius of circular arc  
 $r$  chord distance between points on arc  
 $s$  arc length  
 $\mu$  increment of arc length  
 $a, b$  points on arc  
 $\omega$  angle of chord between points on arc  
 $n$  displacement normal to arc  
 $\delta$  angle of deviation  
 $R$  radius of transformed circle  
 $\epsilon$  difference between circle and near circle angles

$$g = \frac{r_i}{r_t}$$

$$g' = \frac{r_i'}{r_t'}$$

#### Subscripts

- $O$  mean flow  
 $l$  incoming flow  
 $i$  interference on central blade due to presence of external blades  
 $s$  self-induced flow  
 $N$  normal to cascade axis  
 $P$  parallel to cascade axis  
 $T$  total  
 $n$  nose  
 $t$  trailing edge

O,I,II,III zeroth, first, second, and third approximations  
 u,l upper and lower surfaces  
 a,b points on arc

## PROBLEMS IN THE DESIGN OF THIN BLADES

### Problem I

The problem most readily solved is the determination of the shape and setting of thin blades with a prescribed type of vorticity distribution and total vortex strength in a cascade of given solidity for a given direction of the mean flow. The procedure is as follows: a reasonable blade shape and setting are assumed for the zeroth approximation of the iteration process. The stream function and velocity potential on a particular blade of the cascade, which will be referred to as the central blade, are calculated as the sum of those due to the following three flows:

- (1) The given mean flow
- (2) The cascade interference flow, due to the vorticity distribution on all the other blades
- (3) The self-induced flow due to the vorticity distribution along the central blade itself

The assumed shape is then rotated and distorted to make it approximate a streamline in this flow (that is, to make it coincide with a line along which the stream function is constant) and this new shape is used for the cascade blades of the next approximation. Through iteration of this procedure until distortions are too small to affect the flow, the desired blade shape and setting are obtained.

Mean flow.— For convenience, the component of the mean flow velocity normal to the stagger line  $v$  will be considered as unity. The velocity  $V_0$  of the mean flow is then known from its direction. The stream function  $\psi_0$  and velocity potential  $\phi_0$  at a point  $x,y$  on the central blade are then seen from figure 1 to be:

$$\left. \begin{aligned} \psi_0(x,y) &= -V_0(x \sin \alpha_0 + y \cos \alpha_0) \\ \phi_0(x,y) &= -V_0(x \cos \alpha_0 - y \sin \alpha_0) \end{aligned} \right\} \quad (1)$$

where  $\alpha_0$  is the angle of attack of the mean flow with respect to the chord.

Cascade interference flow.— The prescribed vorticity distribution on each blade of the cascade is replaced by a number of discrete vortices, and the induced stream function  $\psi_1$  and velocity potential  $\Phi_1$  are found by using the charts and methods discussed in reference 1.

Self-induced flow.— The stream function induced at a point  $b$  of the central blade by the vorticity distribution on that blade is given by the integral along the blade of the imaginary part of the complex flow function of the distribution, namely

$$\psi_s(s_b) = -\frac{1}{2\pi} \int_{s_n}^{s_t} \gamma(s_a) \log_e r_{ab} ds_a \quad (2)$$

where  $\gamma$  is circulation per unit arc length, and  $r_{ab}$  is the length of the chord between  $b$  and the variable point  $a$ .

As the variable point  $a$  approaches the point  $b$ , the integral becomes improper. If the segment from  $s_b - \mu$  to  $s_b$  is made sufficiently small, that portion of the blade can be considered a straight line and its vorticity uniform. Then  $r_{ab}$  becomes  $|s_b - s_a|$  and  $\gamma(s)$  becomes a constant  $\gamma(s_b)$ . The stream function induced by that segment then is

$$-\frac{\gamma(s_b)}{2\pi} \int_{s_b - \mu}^{s_b} \log_e |s_b - s_a| ds_a = -\frac{\gamma(s_b)}{2\pi} \left[ \mu \log_e \mu - \mu \right] \quad (3)$$

The total self-induced stream function at the point  $b$  is then

$$\begin{aligned} \Psi_s(s_b) = & -\frac{1}{2\pi} \int_{s_n}^{s_b-\mu_1} \gamma(s_a) \log_e r_{ab} ds_a \\ & -\frac{1}{2\pi} \int_{s_b+\mu_2}^{s_t} \gamma(s_a) \log_e r_{ab} ds_a \\ & -\frac{\gamma(s_b)}{2\pi} \left[ \mu_1 - \mu_1 \log_e \mu_1 + \mu_2 - \mu_2 \log_e \mu_2 \right] \end{aligned} \quad (4)$$

Since the function  $\log_e r_{ab}$  is not known analytically for an arbitrarily shaped blade, the integrals of equation (4) are evaluated numerically.

The corresponding integration for the velocity potential requires special care, inasmuch as the contribution of each vortex element  $\gamma(s)ds$  is multivalued. For the present case uniqueness may be provided by using the section of the blade that lies to the right of the vortex element as the branch cut, in which case the potentials contributed by a vortex element situated at a point  $a$  are defined by the angles shown in figure 2. For a point  $b$  to the left of  $a$ , the angles defining the potentials on the upper and lower sides,  $b_u$  and  $b_l$ , are the same. For a point  $b$  on the right side of  $a$ , however, it is necessary to differentiate between  $b_u$  and  $b_l$ ; thus the angle representing the potential on the upper side is designated  $\omega_{ab_u}$ , and that representing the potential on the lower side is designated  $\omega_{ab_l}$ , where, from figure 2,  $\omega_{ab_l} = 2\pi + \omega_{ab_u}$ .

The velocity potentials due to the entire blade at the upper and lower sides of a point  $b$  are then given by

$$\begin{aligned} \Phi_u(s_b) &= \frac{1}{2\pi} \int_{s_n}^{s_b} \gamma(s_a) \omega_{ab_u} ds_a + \frac{1}{2\pi} \int_{s_b}^{s_t} \gamma(s_a) \omega_{ab_u} ds_a \\ \Phi_l(s_b) &= \frac{1}{2\pi} \int_{s_n}^{s_b} \gamma(s_a) \omega_{ab_l} ds_a + \frac{1}{2\pi} \int_{s_b}^{s_t} \gamma(s_a) \omega_{ab_l} ds_a \\ &= \frac{1}{2\pi} \int_{s_n}^{s_b} \gamma(s_a) \omega_{ab_u} ds_a + \frac{1}{2\pi} \int_{s_b}^{s_t} \gamma(s_a) (2\pi + \omega_{ab_u}) ds_a \end{aligned} \quad (5)$$

The average self-induced velocity potential at the point  $b$  is then

$$\begin{aligned}\Phi_s(s_b) &= \frac{\Phi_u(s_b) + \Phi_l(s_b)}{2} \\ &= \frac{1}{2\pi} \int_{s_n}^{s_b} \gamma(s_a) \omega_{abu} ds_a + \frac{1}{2\pi} \int_{s_b}^{s_t} \gamma(s_a) \omega_{abu} ds_a \\ &\quad + \frac{1}{2} \int_{s_b}^{s_t} \gamma(s_a) ds_a\end{aligned}\quad (6)$$

For convenience, a new angle  $\omega_{ab}$  is now defined which is always measured from right to left, irrespective of the position of  $a$  with respect to  $b$ , and for which the following relations then hold:

$$\left. \begin{aligned}\omega_{abu} &= \omega_{ab} && \text{for } s_b > s_a \\ \omega_{abu} &= \omega_{ab} - \pi && \text{for } s_b < s_a\end{aligned}\right\} \quad (7)$$

The average self-induced velocity potential at a point  $b$  is therefore given by substituting relations (7) into equation (6), thus

$$\Phi_s(s_b) = \frac{1}{2\pi} \int_{s_n}^{s_t} \gamma(s_a) \omega_{ab} ds_a \quad (8)$$

Since the angle  $\omega_{ab}$  is not known analytically for an arbitrarily shaped blade, the integral of equation (8) is evaluated numerically.

The choice of a circular arc shape for the initial approximation facilitates the calculation of the self-induced flow, especially when uniform vorticity is specified. The self-induced velocity potential and stream function for constant vorticity on a circular arc are derived in the appendix.

Rotation and distortion of the blade shape.— The sum of the stream functions  $\psi_T = \psi_0 + \psi_s + \psi_1$  on the assumed blade will in general not be the same at every point; that is, the blade will not be a streamline in the complete flow. The flow crosses the



blade at each point at an angle given by the ratio of the local normal velocity to the local average tangential velocity. Thus

$$\delta(s) = \frac{\partial \phi_T / \partial n}{\partial \phi_T / \partial s} = - \frac{\partial \psi_T / \partial s}{\partial \phi_T / \partial s} = - \frac{\partial \psi_T(s)}{\partial \phi_T(s)} \quad (9)$$

where  $\delta(s)$  is the deviation angle measured clockwise, and  $n$  is the coordinate normal to the arc at any point. In order to make the blade follow the streamline, the blade must be distorted so that the direction of each element is changed by this deviation angle. For small deviations, the distortion is effected by a normal displacement given by the integral of the deviation angle along the blade

$$n(s) = \int_{s_n}^{s} \frac{\partial \psi_T(s)}{\partial \phi_T(s)} ds \quad (10)$$

As an intermediate step the given shape may be rotated by the average angle of deviation  $\bar{\delta}$  before the blade shape is distorted. New mean flow and interference velocity potentials and stream functions are then found (the self-induced flow remains the same, however) and the distortions are calculated as just described. In order to minimize the distortions, displacements are taken relative to the displacement at the point where the calculated displacement is the average of the extreme displacements.

If a finite vorticity is required near the tips, infinite slopes appear at the tips (reference 3, p. 10). The finite slopes that are defined by the arbitrary procedure of reference 3 can, however, be adapted to the present problem. The blade shape at the tips given in reference 3 for a similar vorticity distribution can be used, if the ordinates are multiplied by the lift coefficient of the blade based on the average tangential velocity at the tip.

Example I.— As an example of the design procedure outlined, a blade was designed for a cascade of solidity 1.5 such that, with a mean flow direction making an angle of  $40^\circ 54'$  with the normal to the stagger line, it would have uniform vorticity along the blade and a total vortex strength of 1.7321 per blade (based on unit velocity normal to the stagger line and unit cascade spacing). These conditions correspond to a flow coming in at  $60^\circ$  to the normal and leaving normal to the stagger line.

A  $60^\circ$  circular arc (indicated by 0 in fig. 3) with a chord of 1.5 was chosen as the zeroth approximation. The blade angle was taken as  $30^\circ$  to the normal so that the tips were tangent to the incoming and outgoing flow directions. The angle of attack of the mean flow is then  $10^\circ 54'$ . By following the indicated procedure the average angle of deviation was found to be  $7^\circ 31'$ . Rotating the circular arc through this angle and repeating the procedure described gave the shape designated as I in figure 3. The rotation angles for the second and third approximations were  $0^\circ 49'$  and  $0^\circ 9'$ , respectively. The shapes obtained are designated as II and III in figure 3. The angles of deviation  $\delta$  found after rotation are plotted in figure 4. The final blade angle was  $36^\circ 35'$ . The squares of the velocities on the upper and lower sides are plotted in figure 5.

#### Problem II

The procedure of problem I can easily be adapted to the design of thin blades having certain prescribed types of velocity or pressure distributions instead of vorticity distributions. In the second problem the solidity of the cascade, the mean flow direction, and the total vorticity per blade are given, and a thin blade having the prescribed type of velocity distribution over one side is sought. The procedure is somewhat similar to that of the first problem. A reasonable blade shape, blade angle, and vorticity distribution are assumed for the zeroth approximation. The average total velocity potential  $\Phi_T$  is found as in problem I and the average tangential velocity is found from the slope of the curve of  $\Phi_T$  plotted against the distance  $s$  along the blade. This average tangential velocity is now plotted against  $s$  and the prescribed type of velocity distribution on one surface is then plotted on the same graph so that the area between the two curves is equal to half the desired total vorticity. (The possibility of uniquely performing this last step determines whether the type of velocity distribution specified in the problem is one for which a solution can be found by this procedure). The velocity distribution on the other surface may now be plotted such that the average-velocity curve falls midway between it and the curve of the velocity on the first surface. The area between the velocity curves for the upper and lower surfaces then represents the total vortex strength, and the difference in ordinates at each value of  $s$  represents the local vorticity on the blade.

The vortex distribution thus determined is used to find a first approximation to the shape and blade angle by carrying out one step of the procedure of problem I. By assuming the vortex distribution to be unchanged, the total average velocity potential  $\Phi_T$

is then found for this new blade and the average tangential velocity is determined. A new vorticity distribution is then found by the same procedure as before. The process is continued until further changes become inappreciable.

Example II.— By following the procedure outlined, a cascade of solidity 1.5 was designed so that the total vortex strength per blade was 1.7321 in a mean flow making an angle of  $40^{\circ}54'$  with the normal to the stagger line, just as in the first example, but with the velocity on the upper surface uniform over the forward 60 percent of the arc and then decreasing linearly to the mean velocity at the trailing edge.

The blade shape, blade angle, and vortex distribution obtained in example I were chosen for the zeroth approximation. The new vortex distribution was found by plotting the average tangential velocity, as in figure 6, and then finding an upper surface velocity distribution of the prescribed type such that the area between the two curves was 0.866. The vorticity distribution was then twice the difference between the two curves.

The average angle of deviation was found to be  $-1^{\circ}32'$  and the shape after distortion was that designated as I in figure 7. The rotation angles of the second and third approximation were  $-1^{\circ}1'$  and  $0^{\circ}19'$ , respectively, and the shapes obtained are designated as II and III in figure 7. The angles of deviation  $\delta$  found after rotation are plotted in figure 8. The final blade angle was  $36^{\circ}21'$ . The squares of the velocities on the upper and lower sides are plotted in figure 9.

## PROBLEMS INVOLVING A SPECIFIED INCOMING-FLOW DIRECTION

### Problem III

In reference 1 it was shown how, after a solution had been found for a given cascade in a particular mean flow, the conformal transformation of the cascade to a circle could be found; whence the solution for any other specified mean flow, incoming flow, or outgoing flow can be obtained. The present section will discuss the procedure for getting the solution of a given cascade directly when the incoming flow direction, rather than the mean flow direction, is specified. This problem is considered of interest because in experimental cascade studies the incoming flow direction is normally used as a basic parameter rather than the mean flow direction; furthermore, the discussion of this problem will provide a convenient basis for the discussion of the succeeding problem.

Mean flow and total vortex strength.— In the first step, as in reference 1, the conformal transformation of the isolated blade to a circle is determined by the methods of reference 4. The flow field at the isolated blade is now considered as being composed of three superimposed flow fields

(1) A uniform flow of unit velocity, normal to the stagger line (making an angle  $\alpha_N$  with the chord) plus vortices on the blade of total strength  $\Gamma_N$  which maintain the blade a streamline in this flow.

(2) A uniform flow of velocity  $u_0$  to be determined, parallel to the stagger line (making an angle  $\alpha_p$  with the chord) plus vortices of strength  $\Gamma_p$  which maintain the blade a streamline in this flow.

(3) The interference flow due to the vortices that represent all the other blades of the cascade, plus vortices of strength  $\Gamma_i$  which maintain the blade a streamline in this flow. The total vorticity on the blade will then be  $\Gamma_T = \Gamma_N + \Gamma_p + \Gamma_i$ .

By equation (35) of reference 4

$$\Gamma_p = 4\pi R u_0 \sin(\alpha_p + \epsilon_t) \quad (11)$$

where  $R$  is the radius of the transformed circle and  $\epsilon_t$  is the value of the difference between the circle and near-circle angles at the trailing edge. Similarly

$$\Gamma_n = 4\pi R \sin(\alpha_N + \epsilon_t) = -4\pi R \cos(\alpha_p + \epsilon_t) \quad (12)$$

where the relations between the angles  $\alpha_p$  and  $\alpha_N$  and the magnitudes of the normal and parallel velocity components are shown in figure 10.

For the third component a reasonable distribution of vorticity along the external blades is chosen with a total vortex strength that has temporarily been made unity; and the corresponding change of vortex strength on the central blade  $g$  is found by the method of reference 1. The actual vortex strength induced by the external blades  $\Gamma_i$  is the product of  $g$  and the total vortex strength on each blade  $\Gamma_T$ . The following equation then yields the total vortex strength within each approximation:

$$\Gamma_T = \Gamma_T g + 4\pi R \left[ u_0 \sin(\alpha_p + \epsilon_t) - \cos(\alpha_p + \epsilon_t) \right] \quad (13)$$

A second relation between  $\Gamma_T$  and  $u_0$  is given by elementary cascade theory

$$u_0 = u_1 - \frac{\Gamma_T}{2} \quad (14)$$

Simultaneous solution of equations (13) and (14) then gives the zeroth approximation value of the total circulation and of the parallel component of the mean flow  $u_0$

$$\left. \begin{aligned} \Gamma_T &= \frac{4\pi R \left[ u_1 \sin(\alpha_p + \epsilon_t) - \cos(\alpha_p + \epsilon_t) \right]}{1 - g + 2\pi R \sin(\alpha_p + \epsilon_t)} \\ u_0 &= u_1 - \frac{2\pi R \left[ u_1 \sin(\alpha_p + \epsilon_t) - \cos(\alpha_p + \epsilon_t) \right]}{1 - g + 2\pi R \sin(\alpha_p + \epsilon_t)} \end{aligned} \right\} \quad (15)$$

Vorticity distribution.— When the mean flow has been found, the total velocity potential on the central blade and the vorticity distribution are found as in reference 1. With the use of this vorticity distribution to calculate  $g$ , the entire process is repeated to determine a new  $\Gamma_T$  and vorticity distribution. The procedure is continued until further changes are inappreciable. The velocity distribution on the blade is then found by adding the velocity due to the interference to that due to the mean flow, as is done in reference 1, or it may be found directly by differentiating the potential with respect to the distance along the surface.

Example III.— The potential flow was found for a cascade of solidity 1.5 (given shape and blade angle) with incoming flow at  $45^\circ$  to the stagger line. The blade shape was that derived in example I and the blade angle was  $21^\circ 35'$  which gives the same angle of attack with respect to the incoming flow as in example I.

Uniform vortex distribution was assumed for the zeroth approximation. The total vortex strength  $\Gamma_T$  found for that distribution was 1.2302 and the mean flow was at  $21^\circ 3'$ . Successive approximations gave the following values:

Approximation	Vortex strength	Mean flow direction
0	1.2302	21° 3'
I	1.2530	19° 40'
II	1.2457	20° 40'
III	1.2472	20° 38'

The squares of the velocities on the upper and lower surfaces are plotted in figure 11.

#### Problem IV

The procedure of problem III can be readily extended to determine the stagger angle, for given incoming flow direction, at which an airfoil in cascade is at the "ideal" angle of attack.

Ideal angle of attack condition.— The ideal condition for an airfoil is one for which there is a stagnation point at the nose, or for zero thickness, the condition for which air enters tangentially at the leading edge. With regard to the flow in the plane of the circle to which the airfoil transforms, it is the condition for which the same vortex cancels the velocity at both the leading-edge and trailing-edge points.

The strength of the vortex  $\Gamma'_{\Gamma}$  at the center of the circle which cancels the velocity at the leading-edge point is, in analogy to equation (13),

$$\Gamma'_{\Gamma} = \Gamma'_{\Gamma} g' + 4\pi R \left[ -u_0 \sin(\alpha_p + \epsilon_n) + \cos(\alpha_p + \epsilon_n) \right] \quad (16)$$

The procedure of reference 1, modified to cancel the induced velocity at the leading-edge point, is again used to find the factor for this vortex strength induced by the external blades  $g'$ .

The ideal angle of attack condition is then the condition at which  $\Gamma_{\Gamma} = \Gamma'_{\Gamma}$  or  $\Gamma_{\Gamma} - \Gamma'_{\Gamma} = 0$ , where the total induced vortex strengths  $\Gamma_{\Gamma}$  and  $\Gamma'_{\Gamma}$  are found by equations (13) and (16).

Determination of blade angle.— A blade angle  $\beta_I$  is assumed for the first step and the procedure of the first approximation of example III is carried out to obtain  $\Gamma_{IT}$  and  $\Gamma'_{IT}$  and the vorticity distribution corresponding to one of these two values of the total vortex strength is found. With this vorticity distribution assumed on the external airfoils, the calculation is repeated for a second blade angle  $\beta_{II}$ , which is chosen greater or less than  $\beta_I$  accordingly as  $\Gamma_{IT}$  is greater or less than  $\Gamma'_{IT}$ . By interpolating between or extrapolating from the results for those two values of  $\beta$ , a third value of  $\beta$  is found for which  $\Gamma_T - \Gamma'_T$  should be very nearly zero. A calculation at this value of  $\beta$  either should verify that  $\Gamma_T - \Gamma'_T$  is practically zero or should provide the data for a more accurate interpolation or extrapolation.

In the procedure as just described, only one approximation is made for each blade angle; that is, for each  $\beta$  the vorticity distribution found for the preceding  $\beta$  (using either  $\Gamma_T$  or  $\Gamma'_T$ ) is used for the external airfoils. This method should, in general, suffice for satisfactory convergence; in any case, no more than two approximations for each angle should be required.

Example IV.— The blade angle was found for the blade derived in example I such that it would be at the ideal angle of attack in a cascade of solidity 1.5, with incoming flow  $45^\circ$  to the stagger line. The initial blade angle and vortex distributions were those found in example III. Thus  $\beta_I = 21^\circ 35'$  and  $\Gamma_{IT} = 1.2472$ . By equation (16),  $\Gamma'_{IT} = 1.3923$ . Therefore  $\Gamma_{IT} - \Gamma'_{IT} = -0.1451$ . A second calculation, with  $\beta_{II} = 20^\circ 45'$  gave  $\Gamma_{IIT} - \Gamma'_{IIT} = 0.0130$ . Interpolation between the two results indicated that  $\Gamma_T - \Gamma'_T$  would be zero at  $20^\circ 49'$ . A final calculation with  $\beta_{III} = 20^\circ 49'$  verified this fact and gave a vortex strength of 1.2491.

Langley Memorial Aeronautical Laboratory  
National Advisory Committee for Aeronautics  
Langley Field, Va., January 14, 1947

## APPENDIX

SELF-INDUCED FLOW FOR A CIRCULAR ARC WITH  
CONSTANT VORTICITY

The stream function induced at point  $b$  by an element  $ds$  at point  $a$  is (fig. 12)

$$d\psi_s(s_b) = - \frac{\gamma ds_a}{2\pi} \log_e r_{ab} \quad (A1)$$

With the chord and the arc element expressed in terms of the angular position of the points, this equation becomes

$$d\psi_s(\theta_b) = - \frac{\gamma \rho d\theta_a}{2\pi} \log_e \left| 2\rho \sin \left( \frac{\theta_b - \theta_a}{2} \right) \right| \quad (A2)$$

where  $\theta$  is the angular position of the points on the arc, and  $\rho$  the radius of the arc. Or, with  $\frac{\theta_b - \theta_a}{2} = \phi_a$

$$d\psi_s(\theta_b) = \frac{\gamma \rho d\phi_a}{\pi} \log_e \left| 2\rho \sin \phi_a \right| \quad (A3)$$

Equation (A3) is integrated with respect to  $\phi_a$  from  $\phi_n$  to  $\phi_t$  and the first three terms of the series expansion of the integral are retained. The result of this integration, after all terms which do not contain  $\theta_b$  have been omitted (since they add only constants to the stream function) is

$$\psi_s(\theta_b) = - \frac{\rho\gamma}{\pi} \left\{ \left( \frac{\theta_t - \theta_b}{2} \right) \log_e (\theta_t - \theta_b) + \left( \frac{\theta_b - \theta_n}{2} \right) \log_e (\theta_b - \theta_n) \right. \\ \left. + \frac{1}{48} \left[ \theta_b^2 (\theta_n - \theta_t) + \theta_b (\theta_t^2 - \theta_n^2) \right] \right\} \quad (A4a)$$



By adding constants necessary to complete the square in the last term, this equation may be put in the more convenient form

$$\Psi_S(\theta_b) = -\frac{\rho r}{\pi} \left\{ \left( \frac{\theta_t - \theta_b}{2} \right) \log_e (\theta_t - \theta_b) + \left( \frac{\theta_b - \theta_n}{2} \right) \log_e (\theta_b - \theta_n) + \left( \frac{\theta_n - \theta_t}{48} \right) \left[ \theta_b - \left( \frac{\theta_n + \theta_t}{2} \right) \right]^2 \right\} \quad (A4b)$$

In order to find the self-induced average velocity potential  $\Phi_S$  for the circular arc, it is necessary to find the expression for the angle  $\omega_{ab}$  previously defined. From Figure 12 it is seen that

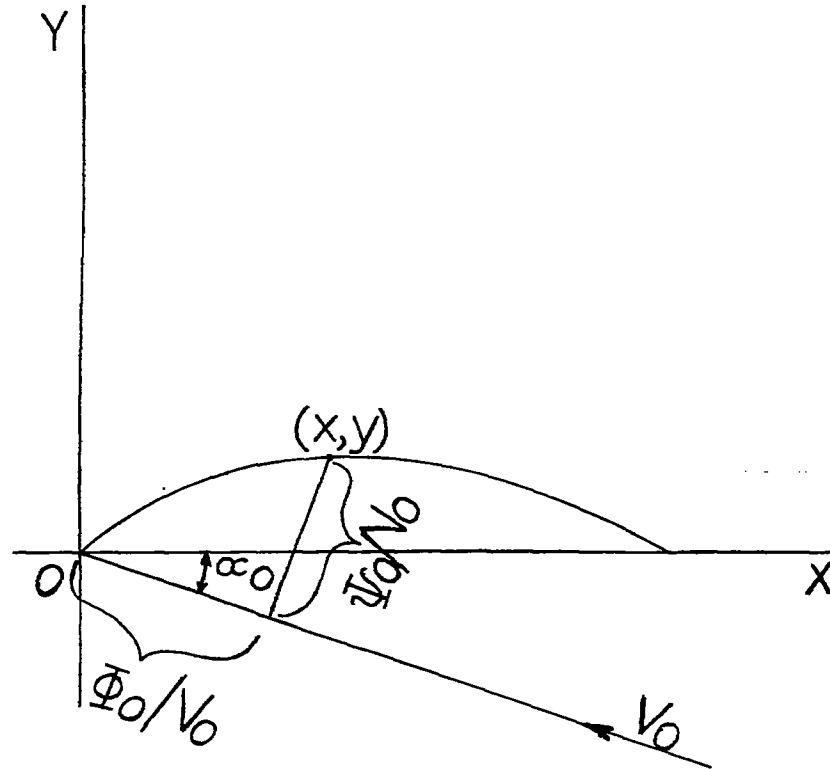
$$\omega_{ab} = \frac{\pi}{2} + \left( \frac{\theta_a + \theta_b}{2} \right) \quad (A5)$$

Substituting this expression into equation (3) and dropping additive constants gives the desired velocity potential

$$\Phi_S(\theta_b) = \frac{\gamma \rho}{4\pi} (\theta_t - \theta_n) \theta_b \quad (A5)$$

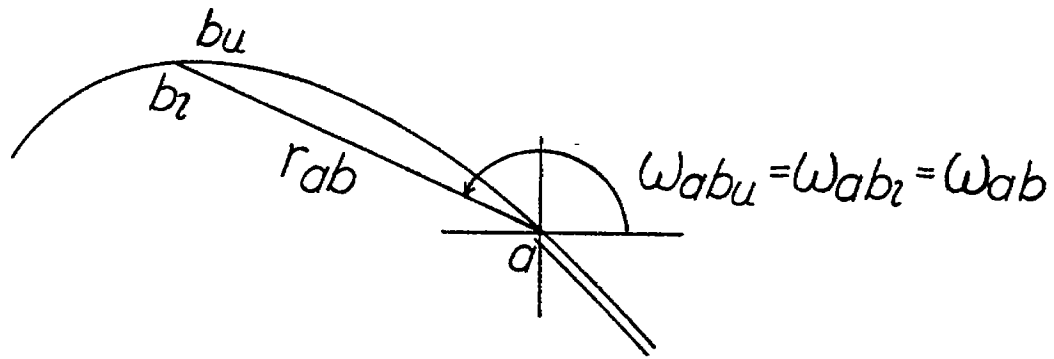
## REFERENCES

1. Katzoff, S., Fim, Robert S., and Laurence, James C.: Interference Method for Obtaining the Potential Flow Past an Arbitrary Cascade of Airfoils. NACA TN No. 1252, 1947.
2. Betz, Albert: Diagrams for Calculation of Airfoil Lattices. NACA TM No. 1022, 1942.
3. Abbott, Ira H., von Doenhoff, Albert E., and Stivers, Louis S., Jr.: Summary of Airfoil Data. NACA ACR No. L5C05, 1945.
4. Theodorsen, T., and Garrick, I. E.: General Potential Theory of Arbitrary Wing Sections. NACA Rep. No. 452, 1933.

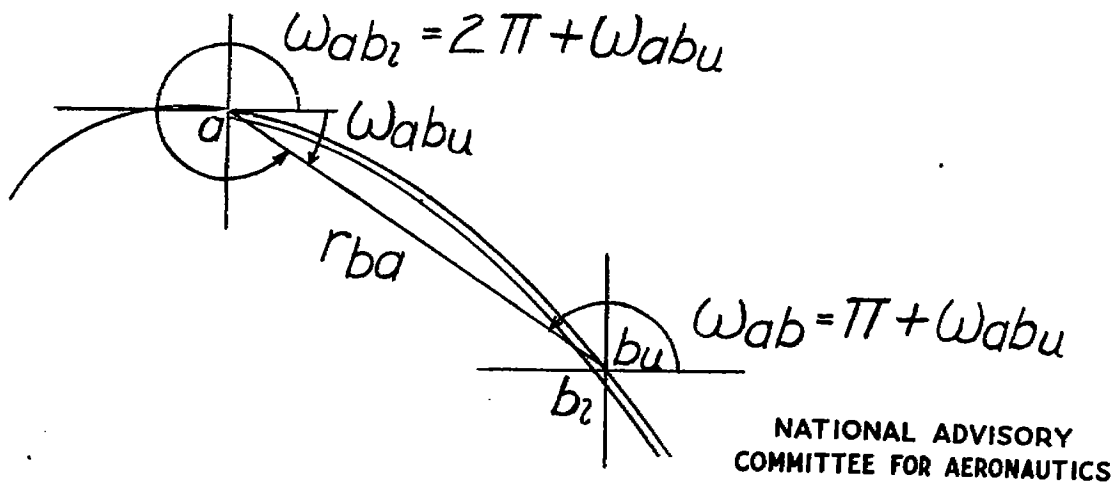


NATIONAL ADVISORY  
COMMITTEE FOR AERONAUTICS

Figure 1.- Potential of the mean flow at a point on the blade.



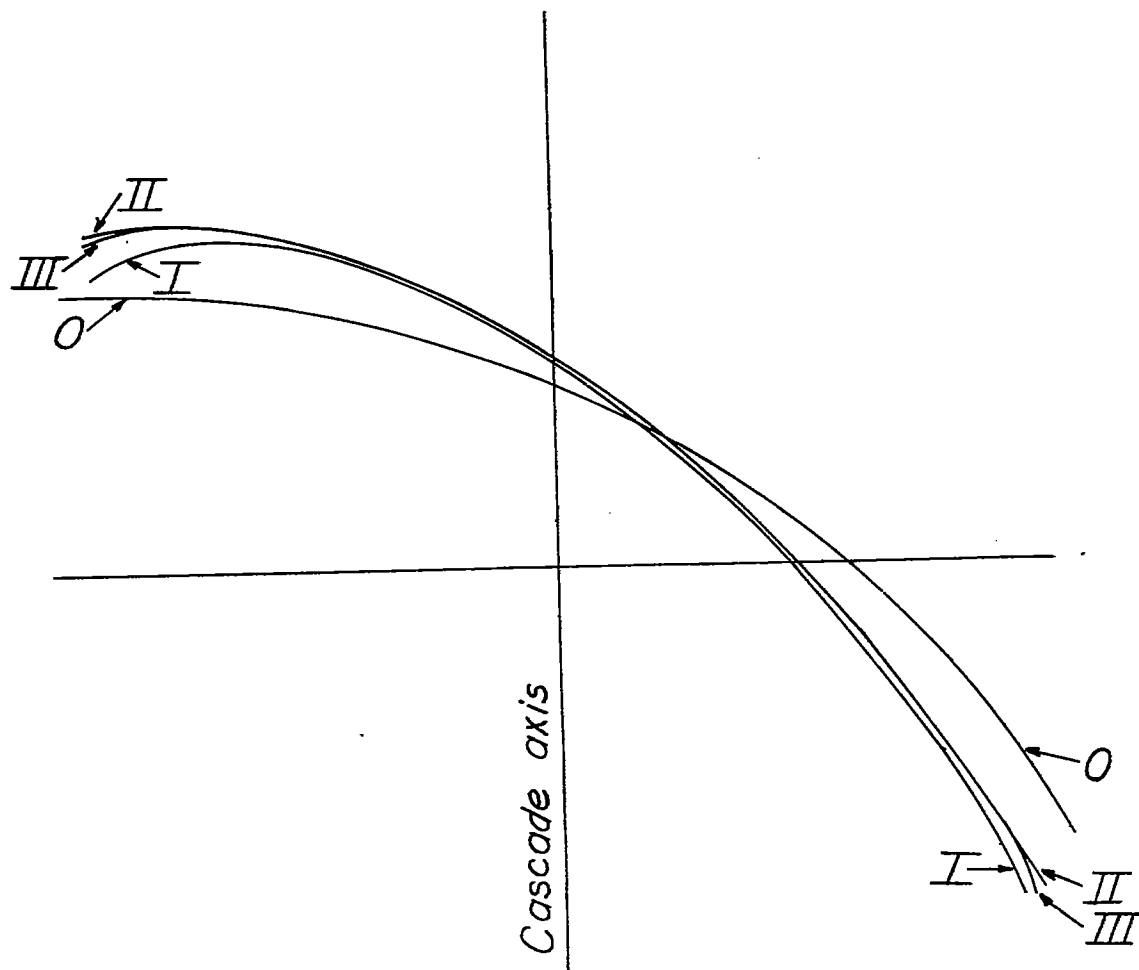
(a)  $s_b < s_a$  (point  $b$  to the left of point  $a$ ).



NATIONAL ADVISORY  
COMMITTEE FOR AERONAUTICS

(b)  $s_b > s_a$  (point  $b$  to the right of point  $a$ ).

Figure 2.- Angles defining self-induced potentials on upper and lower surfaces at point  $b$  due to vortex at point  $a$ .



NATIONAL ADVISORY  
COMMITTEE FOR AERONAUTICS

Figure 3.- Shape and setting of blade used for zeroth approximation of example I, and of blades derived in the subsequent approximations.

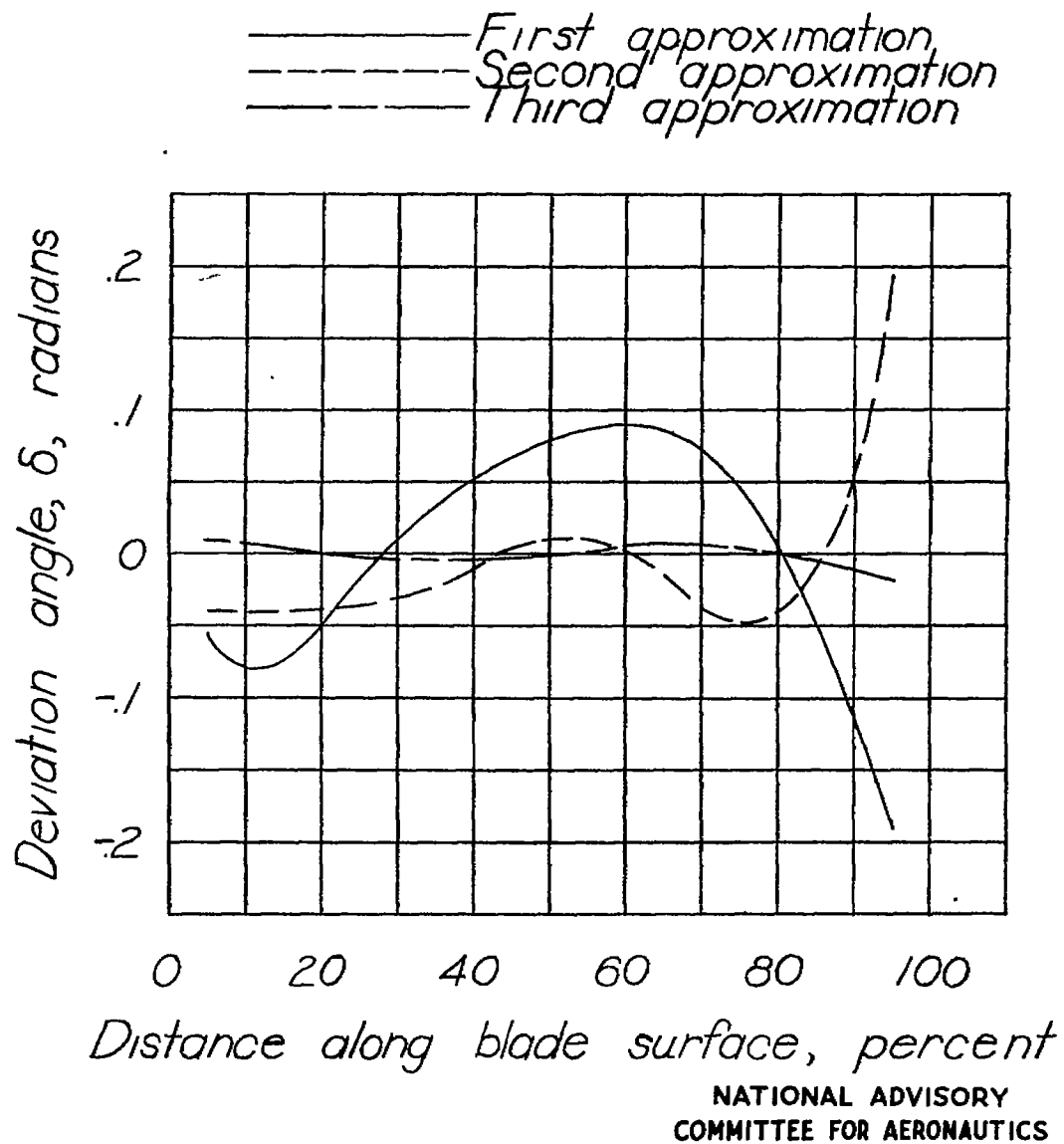
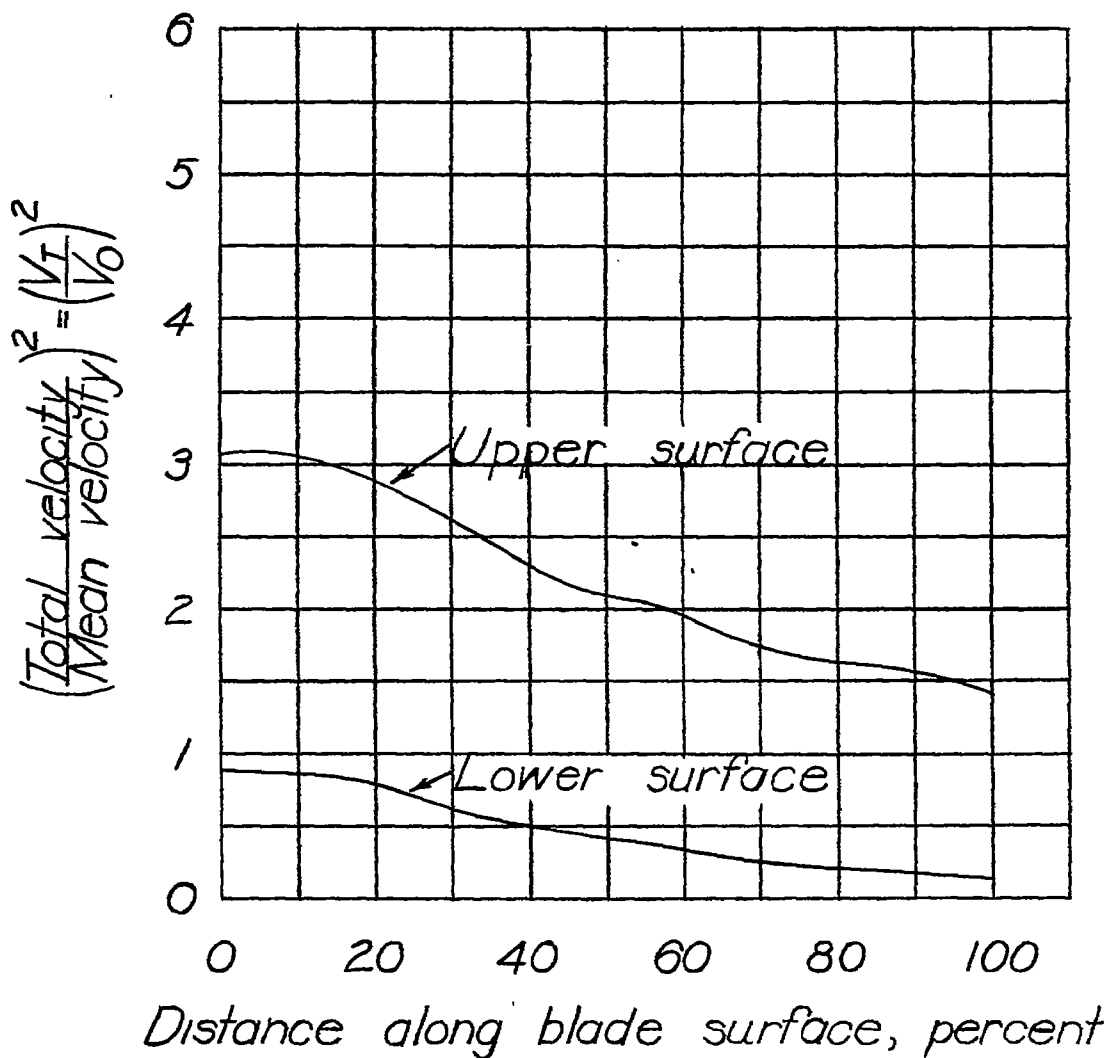
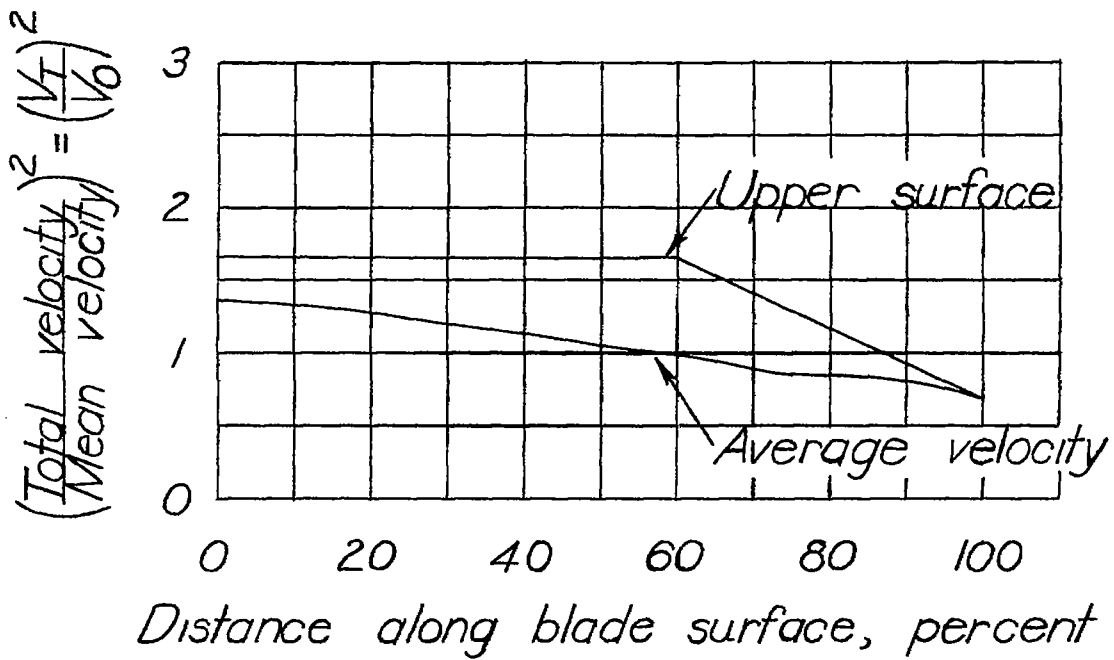


Figure 4.- Deviation angles between arc and streamline for the three approximations of example I, showing rate of convergence.



NATIONAL ADVISORY  
COMMITTEE FOR AERONAUTICS

Figure 5.- Pressure distribution on airfoil derived in example I.



NATIONAL ADVISORY  
COMMITTEE FOR AERONAUTICS

Figure 6.- Average and top surface velocities for example II.



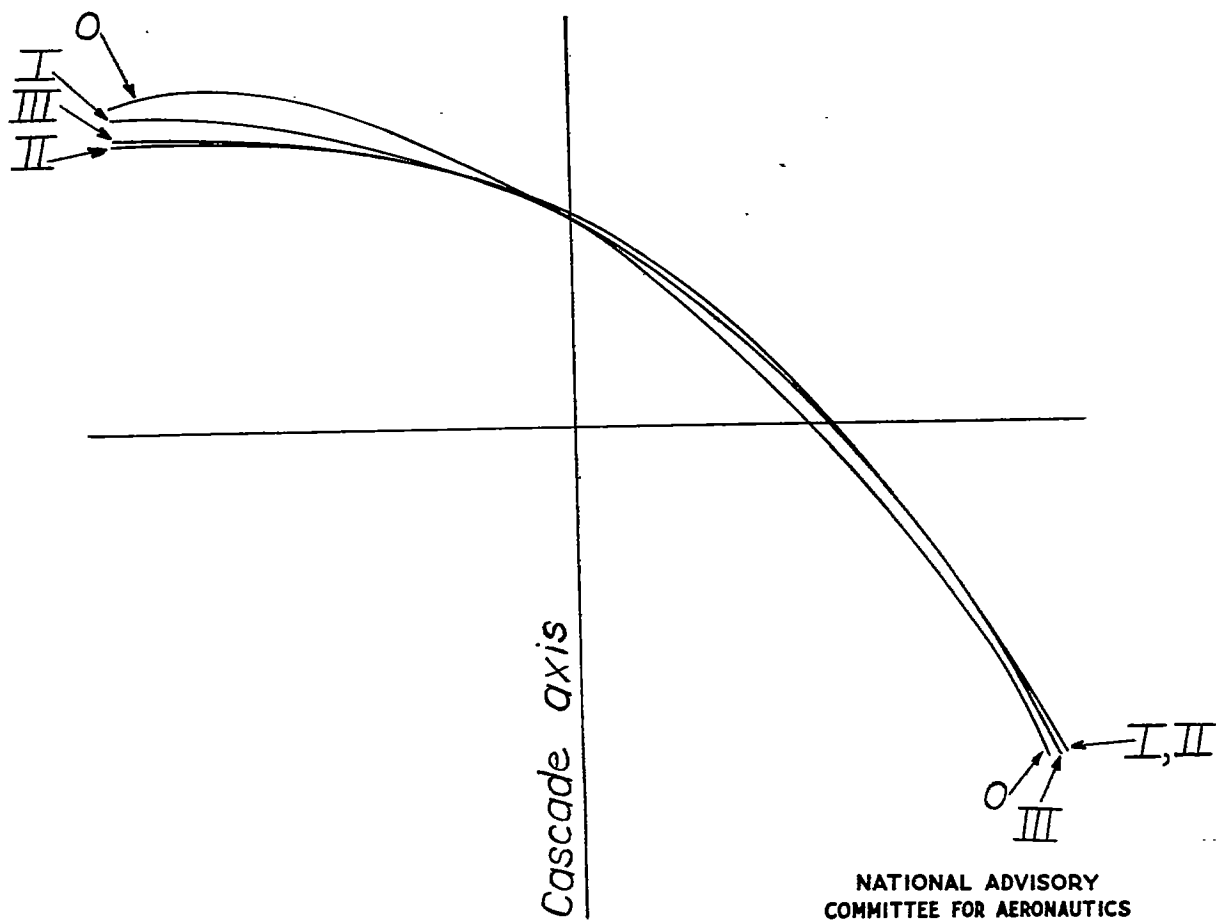


Figure 7.- Shape and setting of blade used for zeroth approximation of example II, and of blades derived in the subsequent approximations.

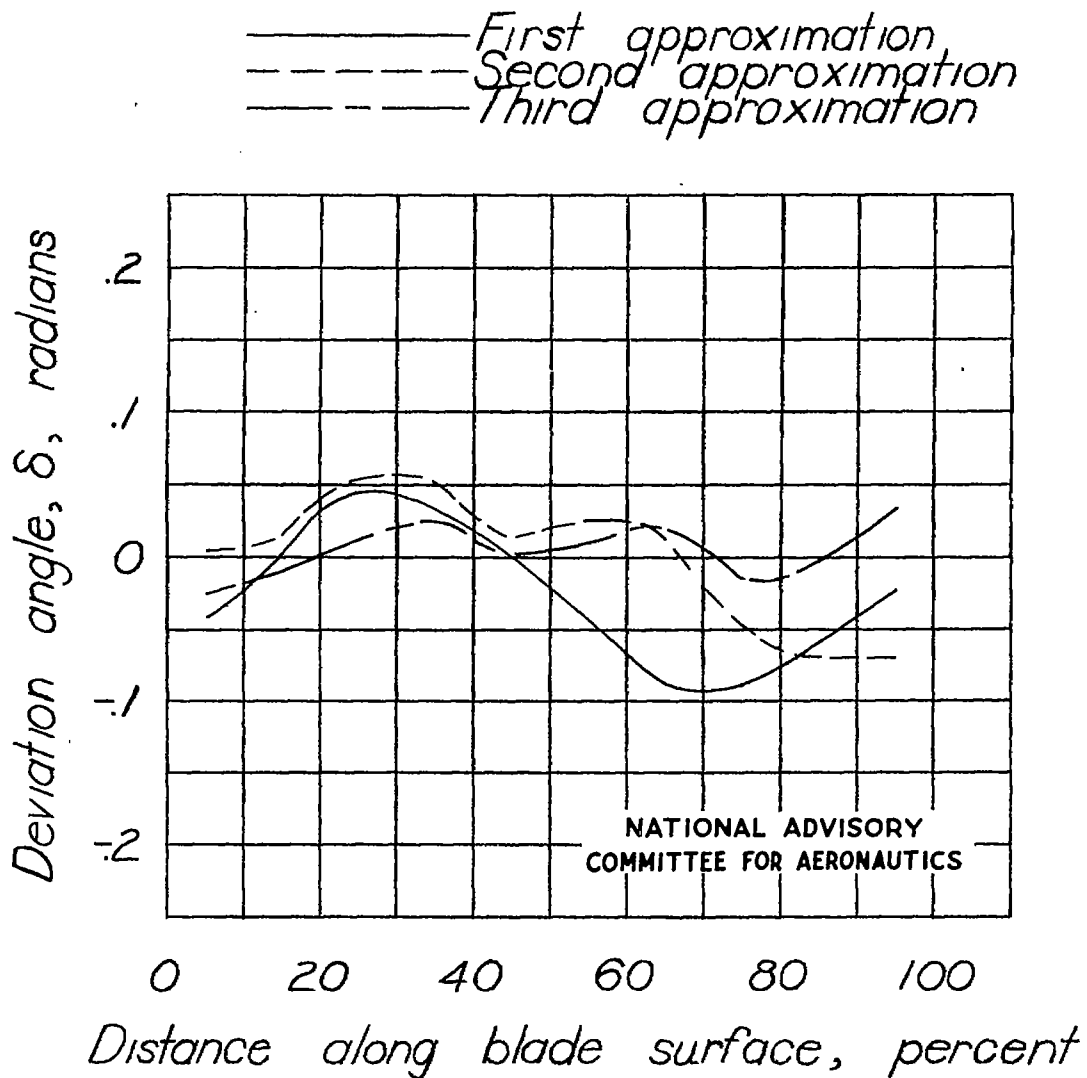


Figure 8.- Deviation angles between arc and streamline for the three approximations of example II, showing rate of convergence.

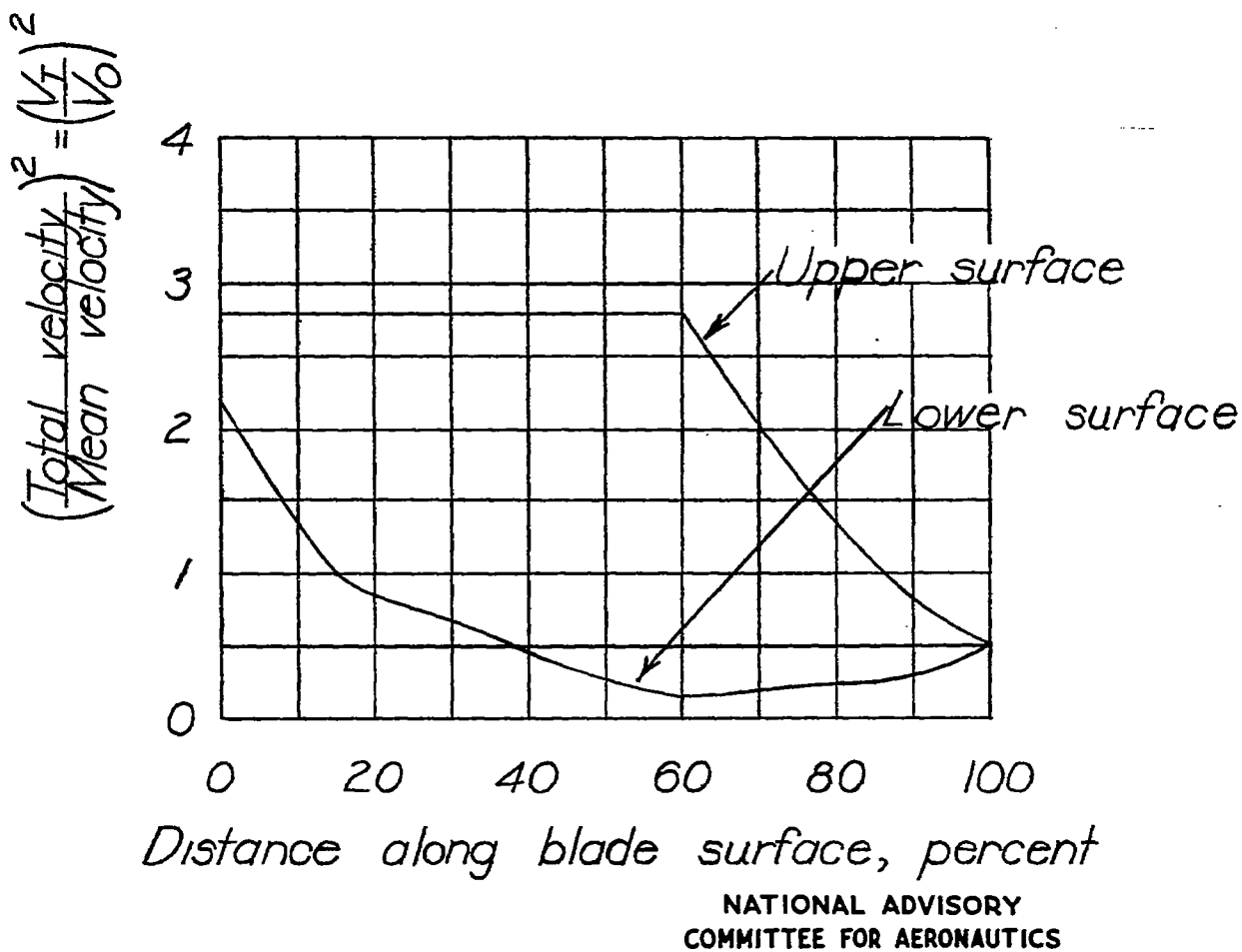


Figure 9.- Pressure distribution on airfoil derived in example II.

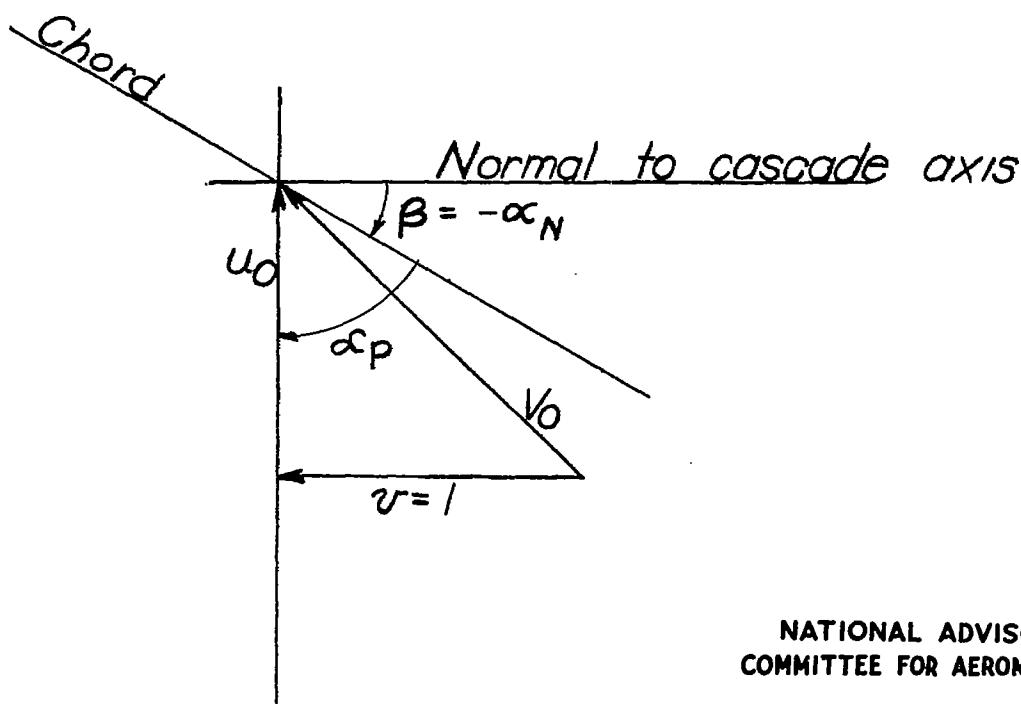
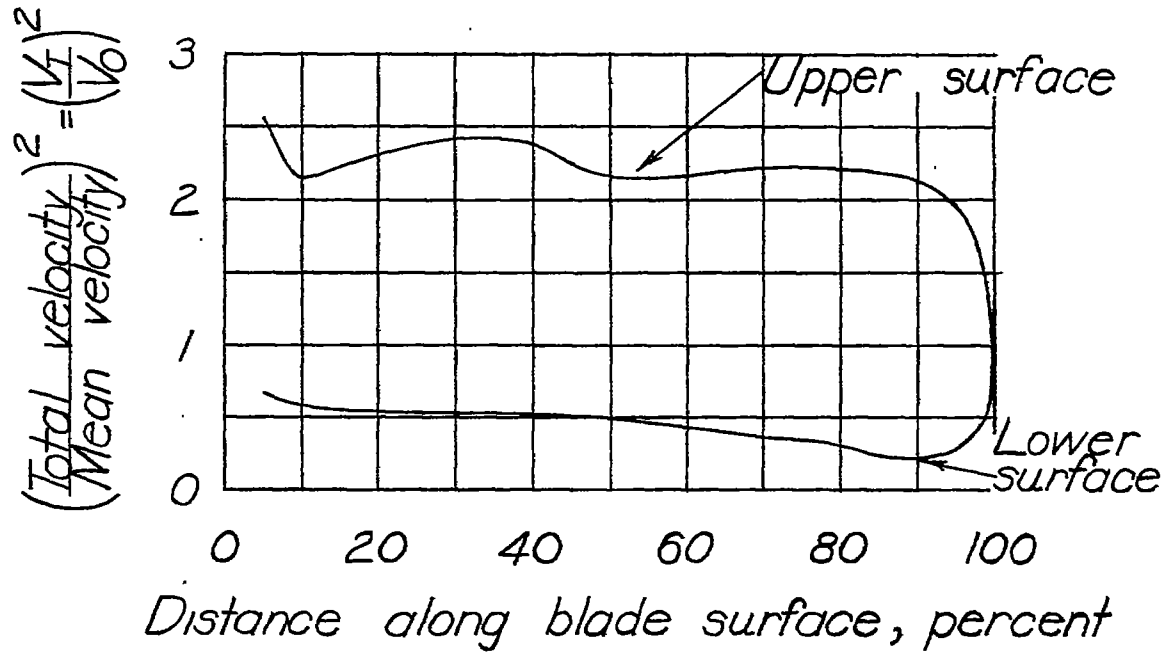
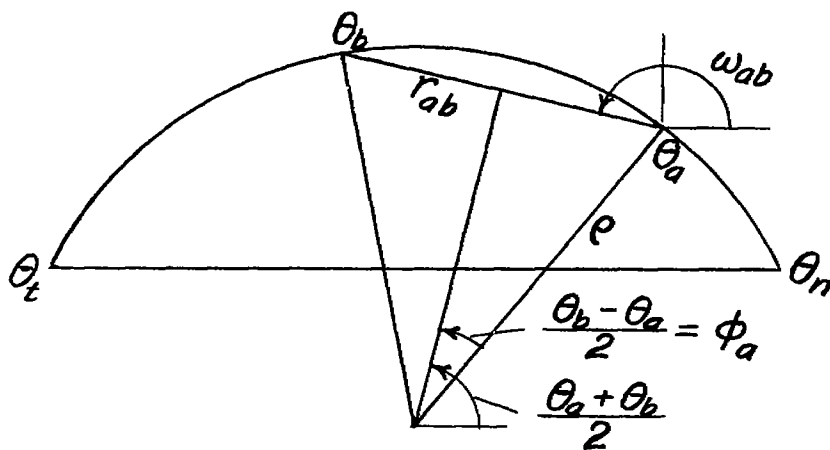


Figure 10.- Definitions of angles and velocities for example III.



NATIONAL ADVISORY  
COMMITTEE FOR AERONAUTICS

Figure 11.- Pressure distribution on airfoil in example III.



NATIONAL ADVISORY  
COMMITTEE FOR AERONAUTICS

Figure 12.- Definitions of angles and distances for derivation of self-induced potential and stream function on circular arc.